doi:10.2533/chimia.2017.124 Chimia 71 (2017) 124–129 © Swiss Chemical Society

Metabolic Profiling of Cells in Response to Drug Treatment using ^{1}H High-resolution Magic Angle Spinning (HR-MAS) NMR Spectroscopy

Martina Vermathen*[a], Gaëlle Diserens[b], Peter Vermathen[b], and Julien Furrer*[a]

Abstract: High-resolution magic angle spinning (HR-MAS) is an NMR technique that provides access to well resolved liquid-like ^{1}H NMR spectra of semi-solid samples. Therefore, ^{1}H HR-MAS NMR spectroscopy has become an important tool for the direct analysis of biological samples such as tissues and cells in a mostly non-destructive way. Here, we focus on the application of HR-MAS NMR combined with multivariate statistical methods used for metabolic profiling of cells and in particular for the study of cellular metabolic responses to drug exposure. The principles of HR-MAS and the metabolomic approach are briefly described. As an example, a study on the metabolic response of different cell types towards treatment with a highly cytotoxic hexacationic ruthenium metallaprism as potential anti-cancer drug is presented. Specific metabolites and metabolic pathways are suggested to be associated with the cellular response. The study demonstrates the potential of HR-MAS metabolomics applied to cells for addressing the intracellular processes involved in the treatment with organometallic drugs.

Keywords: Cells · HR MAS NMR · Metabolic profiling · Ruthenium

Introduction

Bioorganometallic Chemistry and Analytics

The term *bioorganometallic chemistry* is literally the study of biologically active molecules that contain carbon directly bonded to metals or metalloids. As such, bioorganometallic chemistry is a subset of bioinorganic chemistry and encompasses various fields such as organometallic chemistry, biochemistry, and medicine.[1] In particular, the study of the fates of synthetic organometallic compounds in biological environments can be considered as one of its most important aspects.[1]

The search for improved organometallic drugs continues with the goals of reducing the toxic side effects and broadening the spectrum of activity to resistant tumors and metastasis, but also to resistant bacteria and parasites.[2] If we consider the field of anticancer research, a major focus of current research is in the investigation of new organometallic compounds that act by a different mechanism compared to platinum compounds to achieve a different profile of activity.[3–5] Current knowledge of the mechanism of action of organometallic drugs relies on powerful analytical techniques. Some of these techniques are described in other articles of this issue, and selected examples showing the knowledge that can be gained are illustrated.

NMR methods have undoubtedly proved useful in the investigation of organometallic drugs, especially of platinum drugs.[6] Both ^{195}Pt and ^{15}N NMR were used in early studies and made a major contribution in the understanding of the molecular mechanism of action of cisplatin from model studies involving reactions with amino acids and nucleotides.[7] However, these NMR studies were limited by the fact that the actual physiologically relevant conditions could at best be only approximately mimicked. A new technique, high-resolution magic angle spinning (HR-MAS) NMR Spectroscopy was introduced two decades ago and has opened new avenues for the study of molecules that belong neither to the liquid nor to the solid state but which lie somewhere between the two, typically cells and human or animal tissues.[8]

HR-MAS NMR Spectroscopy

The HR-MAS NMR spectroscopy technique[9] was first exclusively used for the characterization of compounds obtained from solid-phase synthesis directly attached to their solid support.[8,10–12] Briefly, the technique is derived from solid state NMR spectroscopy and involves swelling the sample with an appropriate solvent to reintroduce enough mobility, and then using the magic angle spinning (MAS) technique to reduce the NMR linewidths of samples.[9]

Indeed, the dipolar and the chemical shift Hamiltonians are composed of a spin part, which can be manipulated by pulse sequences, and of a spatial part ($1–3\cos^2\theta$), θ being the angle between the internuclear vector and the external magnetic field, which can be manipulated by the sample rotation.[13] The term ($1–3\cos^2\theta$) vanishes in solution, because of the fast molecular reorientations (Brownian motion). It can also vanish in solid state or for 'soft' samples when the sample is spun rapidly at a special angle, the so-called magic angle, which is equal to 54.7°.[13] However, for being really efficient and for obtaining sharp 'liquid-like' resonances, the speed of rotation must be at least equal to the magnitude of the dipolar interaction and of the chemical shift anisotropy. For protons, fortunately, the chemical shift anisotropy is weak, and the swelling of the sample or the soft nature of medical samples (cells,

*Correspondence: Dr. M. Vermathen, Dr. J. Furrer
E-mail: martina.vermathen@dcb.unibe.ch, julien.furrer@dcb.unibe.ch
[a]Department of Chemistry and Biochemistry University of Bern, Freiestrasse 3 CH-3012 Bern, Switzerland
[b]Departments of Clinical Research and Radiology University and Inselspital Bern, Switzerland

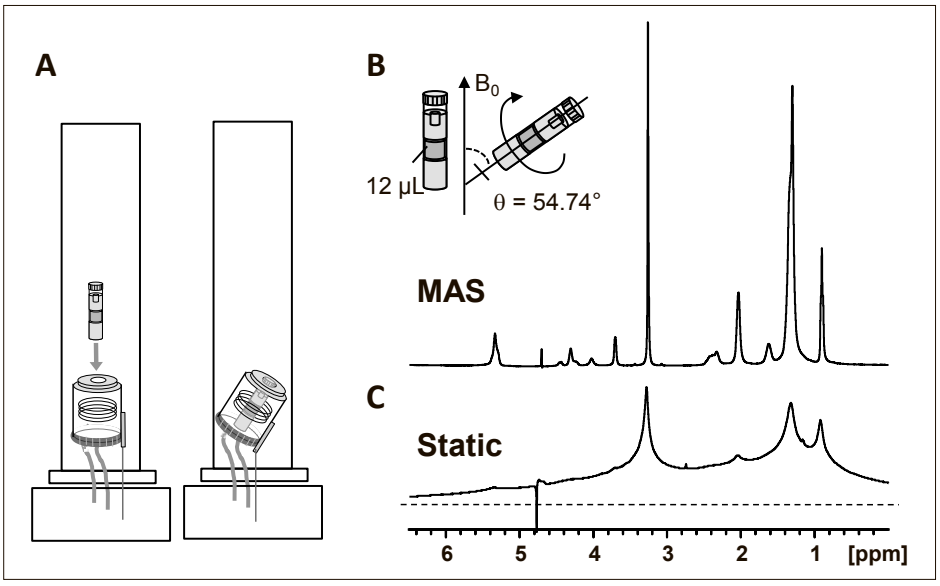

Fig. 1. A: Scheme of an NMR probe with HR-MAS stator in vertical and in magic angle position, ^{1}H NMR spectrum (500 MHz) of large 1,2-dioleoyl-*sn*-glycero-3-phosphocholine (DOPC) vesicles in D_2O acquired with B: magic angle spinning and C: classical liquid state NMR spectroscopy.

tissues) reintroduces enough mobility so that the dipolar interactions between the spins never exceed a few kHz.[8,9]

The reason for the success of HR-MAS is precisely that MAS has the unique property of averaging the large magnetic field gradients present in such heterogeneous samples to zero.[8] Under such conditions, the sample behaves very much like a liquid, and standard liquid-state NMR experiments can be employed to identify and characterize molecules of the soft material. There are many applications of HR-MAS and it is not limited to the study of compounds issued from solid-phase synthesis. Important current applications include the characterization of polymers,[14] lipids[15,16] and biological tissues.[17–19]

Fig. 1A depicts a scheme of an NMR-probe with the HR-MAS stator and rotor containing the sample. Comparison of the ^{1}H NMR spectra shown in Fig. 1B (acquired with HR-MAS) and Fig. 1C (acquired with classical liquid-state NMR) visualizes the resonance narrowing effect of MAS applied to the same sample, exemplified here for a suspension of phospholipid vesicles in D_2O.

Metabolic Profiling of Cells

Metabolic profiling of cells involves the description of the entire range of small molecules covered by the analytical method of choice. The most frequently applied methods for metabolic profiling of tissue or cells are mass spectrometry (MS) combined with chromatography and ^{1}H NMR spectroscopy.[20] Typically, extracts of the biological material have to be prepared prior to analysis. In contrast, the HR-MAS technique allows direct access to the ^{1}H NMR spectra of intact living cells without the need of extraction or separation. This is possible because of the above mentioned MAS-induced minimization of resonance line broadening effects caused by the inherent chemical and physical heterogeneities present in cells, which behave as 'semi-solid' samples. The resulting well resolved small metabolite proton spectra thus represent a unique chemical fingerprint of the cells. Due to the complexity of the metabolite spectra the quantitative analysis is often combined with multivariate statistical methods leading to the field of the so-called 'metabolomics' or 'metabonomics'.[21] The metabolomic approach enables the untargeted detection of even small metabolite alterations caused by specific diseases or following any type of intervention such as drug exposure or specific growth conditions during cell culture. It involves both unsupervised and supervised chemometric tools. Among the unsupervised methods, principal component analysis (PCA) and hierarchical clustering analysis (HCA) are often employed to detect similarities between samples and to identify outliers.[22] Supervised methods employ prior knowledge, *e.g.* the assignment to drug treated and control samples. Typically, partial least squares discriminant analysis (PLS-DA) is applied to the data in order to build classification models for identifying metabolites responsible for separation of the groups.

The chemometric approach applied to the global metabolic profile of cells is thus a powerful tool for finding biomarker components specific for disease or drug response.[23,24] Likewise, it can reveal potential metabolic targets of drugs following cell uptake,[25] or pathways associated with cellular drug response.[26] Consequently, HR-MAS NMR-based metabolomics of cells has found its way into the study of organometallic drugs. Metabolomic studies involving various tumor cell lines exposed to cisplatin have been performed to gain insight into the mechanisms of action on a molecular basis inside the cell.[26–28] The reported cisplatin-induced metabolic cell response included the onset of apoptosis, alterations in lipid metabolism regulation, oxidative stress and DNA-related defense mechanisms.[26,27] Glycosylated uridine-diphosphate (UDP) compounds[26,28,29] as well as unsaturated triglycerides[29] were suggested as biomarkers for cisplatin treatment response predicting cell death.

Organometallic ruthenium complexes have gained much interest as promising alternative drug candidates for the treatment of cancer. This is mainly due to their high affinity for cancer cells combined with low cytotoxic concentrations even against cisplatin-resistant cell lines. The research in our group has focused on a series of multinuclear water-soluble arene ruthenium prisms and their interactions with various biomolecules.[30–34] The HR-MAS-based metabolic profiling approach outlined in this review was applied in order to learn more about potential intracellular pathways involved in the cytotoxic mechanism.[35] For this, three different cell lines were used, human ovarian carcinoma cells which were either sensitive towards cisplatin treatment (A2780 cells) or which have developed cisplatin resistance (A2780cisR cells) as well as human embryonic kidney cells (HEK-293 cells).

^{1}H HR-MAS NMR Spectra of Cells

The analysis of living systems poses challenges on the preparation protocols with respect to maintaining integrity and authenticity of the material while at the same time achieving highly reproducible data. These protocols may involve careful freezing of the cell material with cryoprotectants, lysis of the cells in order to stop metabolism[36,37] or additional heating steps to yield stable samples for measurements of extended time periods.[36] As biological processes such as enzymatic reactions are still ongoing in living cell material, their analysis therefore requires highly standardized experimental protocols to be performed constant in time. The workflow pursued for the samples described here is schematically represented in Fig. 2. Cells were seeded and equilibrated in culture for 24 h before

the culture medium was exchanged by medium either containing the drug dissolved in a small amount of DMSO or only the solvent (DMSO) for control samples. The incubation lasted 24 h or 72 h until the medium was removed. Harvesting of cells included trypsinization and subsequent addition of serum to detach the adherent cells. Following several washing and centrifugation steps of the cell suspension the pellet was finally taken up in freezing medium containing 10% DMSO as cryoprotectant for storage at –80 °C. Samples were thawed, washed and finally taken up in D_2O-based phosphate buffered saline (PBS) shortly before HR-MAS NMR measurement. In this way, each culture flask gave rise to one sample containing approximately 1–5x10^6 cells suspended in 12 µL PBS (D_2O, pH 7.4). To account for sufficient statistical power, eight replicates were prepared for control samples and ten replicates for drug treated samples for each cell line and each incubation time (24 h, 72 h).

In Fig. 3, a representative ^{1}H HR-MAS NMR spectrum of a cell suspension obtained from A2780 ovarian carcinoma cells is shown. The spectrum is divided into the aliphatic region from 0.5 ppm to 4.4 ppm (Fig. 3A) and into the aromatic region between 5 ppm and 8.6 ppm (Fig. 3B). It was acquired with a MAS rate of 3 kHz at a temperature of 37 °C. Typically, pulse sequences applied for metabolic profiling of biological material include water saturation techniques and relaxation editing in order to suppress broad resonances derived from macromolecules with short T_2 relaxation times such as proteins or polysaccharides.[18] The spectrum shown in Fig. 3 was recorded with a Carr–Purcell–Meiboom–Gill (CPMG) pulse sequence (*cpmgpr*, Bruker) used as T_2-relaxation filter. Resonance assignment of complex cell metabolite spectra is based on the combined information obtained from additional 2D correlation spectra (*e.g.* HR-MAS TOCSY), comparison with data bases (*e.g.* human metabolome database, HMDB[38,39]), literature values[20,35,37] and additional spiking with reference compounds.[40] The most prominent peaks in the aliphatic region (Fig. 3A) derive from lipids (Lip) and choline-containing compounds (Cho, PC, GPC) indicating an intracellular mobile lipid pool as for example present in lipid droplets.[15] Typical small metabolites detectable in the aliphatic region of cell spectra are amino acids like leucine (Leu), valine (Val), isoleucine (Ile), glutamine (Gln) and glutamate (Glu) as well as the tripeptide glutathione (GSH) and other organic compounds like lactate (Lac), acetate (Ac) or creatine (Cre). In the spectral region between 5 ppm and 8.5 ppm (Fig. 3B) multiple resonances

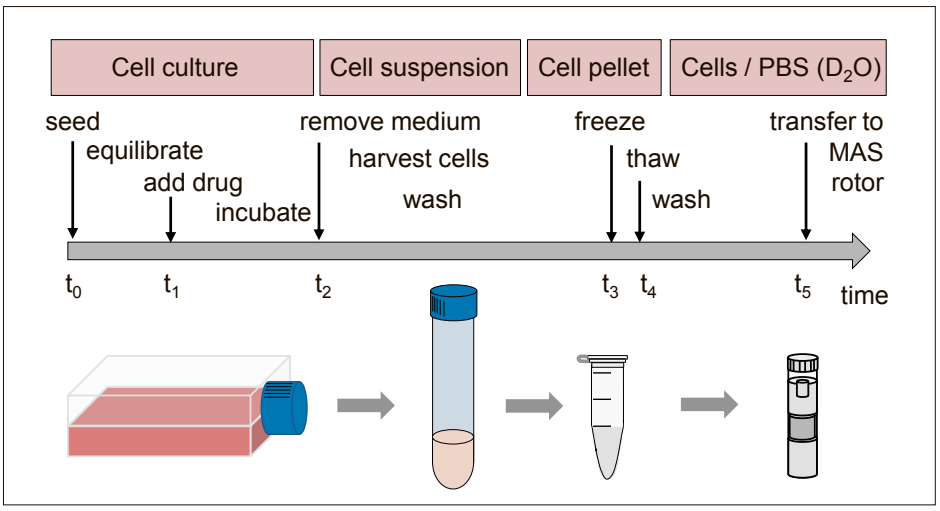

Fig. 2. Workflow for the preparation steps at defined time points (t_0 – t_5) of cell suspensions for HR-MAS NMR measurements.

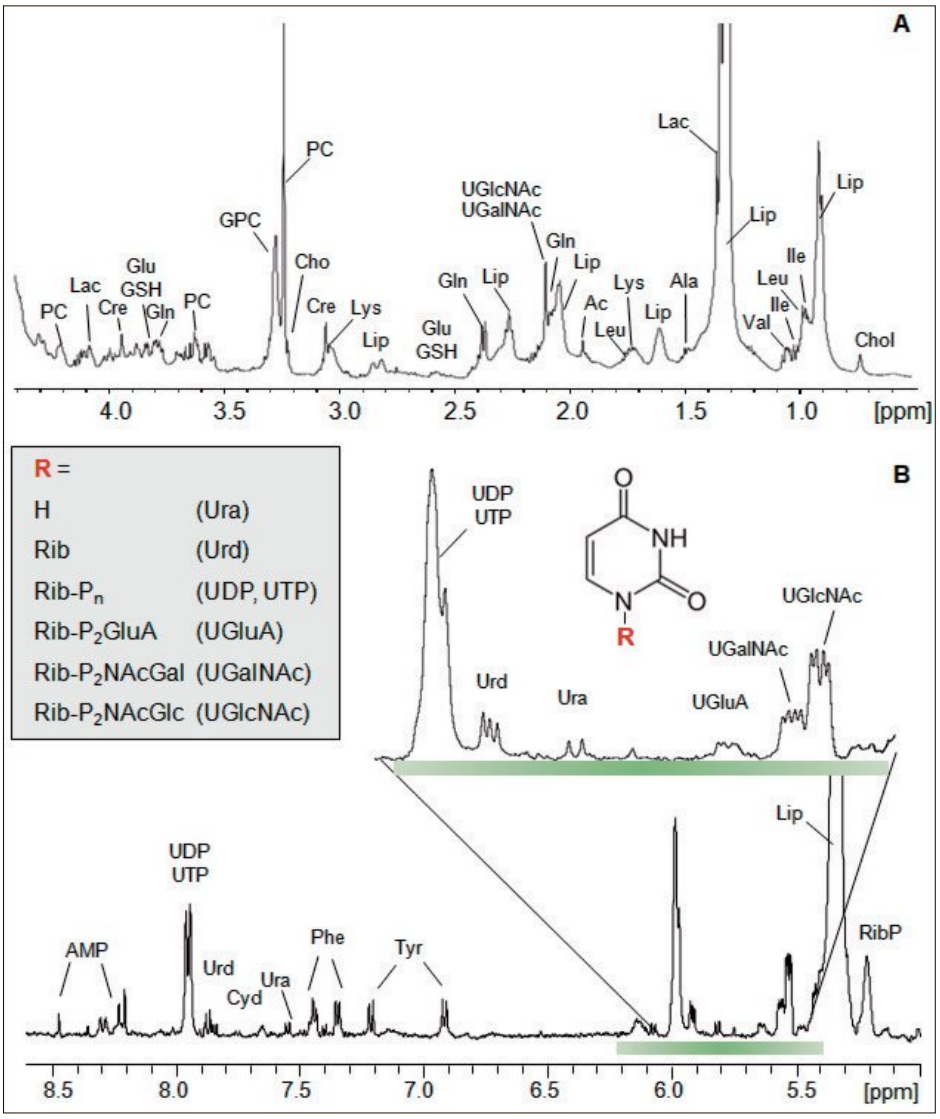

Fig. 3. ^{1}H HR-MAS NMR spectrum of A2780 cells in PBS (D_2O, pH 7.4) acquired at 500 MHz, T = 37 °C, 3 kHz MAS, and a *cpmg*-pulse sequence with water saturation. A: expansion of the aliphatic region, B: expansion of the aromatic region. Resonance assignments: Ac: acetate, Ala: alanine, AMP: adenosine-monophosphate, Cho: choline, Chol: cholesterol & esters, Cre: creatine, Cyd: cytidine, Gln: glutamine, Glu: glutamate, GPC: glycerophosphocholine, GSH: glutathione, Ile: isoleucine, Lac: lactate, Leu: leucine, Lip: lipid, Lys: lysine, PC: phosphocholine, Phe: phenylalanine, RibP: ribose-5-phosphate, Tyr: tyrosine, UDP/UTP: uridine-di-/tri-phosphate, UGalNAc: UDP-N-acetyl-galactosamine, UGlcNAc: UDP-N-acetyl-glucosamine, UGluA: UDP-glucuronic acid, Ura: uracil, Urd: uridine, Val: valine.

originate from nucleotides mainly derived from the pyrimidine base uracil (Ura). The nucleotide sugars (UGlcNAc, UGalNAc, UGluA) give rise to characteristic multiplets (at around 5.5 ppm) due to coupling of the anomeric sugar protons with phosphate nuclei.[40] They play key roles in intracellular enzymatic glycosylation processes as sugar donors to form glycolipids, glycoproteins or polysaccharides. Taken together, the detectable small metabolites are part of specific metabolic pathways or reactions as educts, intermediates or products and at large provide a chemical snapshot of the cells.

The Metabolic Profile of Untreated Cells — PCA of Control Cells

In Fig. 4, a three-dimensional PCA plot for all untreated control cell samples is shown. Each data point represents one ^{1}H HR-MAS NMR spectrum. The relative amount of variance explained by each PC component is given in brackets. Prior to PCA, the processed ^{1}H HR-MAS cell spectra were subdivided into 97 individually sized buckets (X-variables) minimizing resonance overlap for every single bucket and excluding noise regions. With 8 cell samples for each cell line (A2780, A2780cisR, HEK-293) and 2 different incubation times (24 h, 72 h) a total number of 48 spectra (Y-variables) were analyzed resulting in an XY-data matrix of 97 × 48. PCA reduces the complexity of the matrix by projecting the data into a two- or three-dimensional space to explain the variance along the projected PC components. It is a means to visualize the similarity between samples or their magnitude of variance, respectively, in an unsupervised manner. The 95% confidence ellipsoids mainly reflect the intrinsic variations inherent to biological material but also variations due to sample handling and measurement. A clear clustering of the samples according to cell line and incubation time was obtained. The similarity between samples of the same group confirmed a good reproducibility of the data and suggested cell line specific metabolic profiles such as those caused by different genetic expressions. Accordingly, molecular signatures of cells accessible through HR-MAS NMR metabolomics have been used for phenotyping of tumor cells[41] and diseases.[42] Another important finding was the separation of cells from the same cell line depending on incubation time, which underlines the importance of standardized timed growth conditions. Nutrient consumption and increased cell density during cell culture caused metabolic alterations most pronounced for A2780 and HEK-293 cells (Fig. 4).

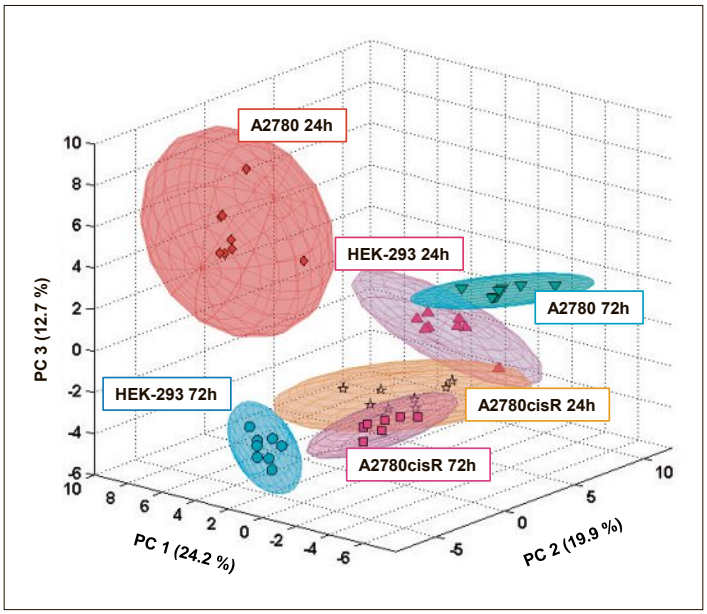

Fig. 4. PCA scores plot for the first three PC-components calculated for the ^{1}H HR-MAS spectra of untreated (control) cell suspensions obtained from A2780, A2780cisR, and HEK-293 cell cultures after 24 h and 72 h incubation time. The 95% confidence ellipsoids are displayed for each group.

Example: Effects of a Ruthenium Metallaprism against Cells

The hexanuclear ruthenium metallaprism $[(p\text{-cymene})_6Ru_6(tpt)_2(dhnq)_3]^{6+}$ ([**1**]) shown in Fig. 5 emerged as highly cytotoxic against A2780, HEK-293, and even the cisplatin-resistant A2780cisR cells with IC_{50} values below 1 μM. To gain insights into the metabolic pathways associated with the cytotoxic effect of [**1**], the metabolic response of A2780, A2780cisR, and HEK-293 cells was studied following treatment with [**1**].[35]

PLS-DA was applied to the data to obtain a model for distinguishing control cells from drug-treated cells. The PLS-DA scores plots are displayed in Fig. 6 for an incubation time of 24 h. In these models drug-treated (shown in red) and control samples (shown in blue) were well separated mostly along the first latent variable (LV-1) for all three cell lines. Controls gave rise to negative scores on LV-1 while cells exposed to [**1**] gave rise to positive LV-1 scores. The distinguishing features were most pronounced for A2780 cells (Fig. 6C), followed by A2780cisR (Fig. 6A) and HEK-293 cells (Fig. 6D). To derive meaningful information from the PLS-DA models the corresponding so-called loading plots were analyzed. An example is shown in Fig. 6B. It displays the load values for all X-variables (buckets) according to their impact on the first PLS-DA component for the PLS-DA scores plot comparing A2780cisR control and drug-treated cells (Fig. 6A). Buckets with high positive values are displayed in red and buckets with high negative values are displayed in blue. The corresponding metabolites can be considered as strong contributors to the discrimination between sample groups. Metabolites giving rise to multiple NMR resonances or buckets should thus result in correlated load values. Exposure of [**1**] to A27808cisR cells resulted in increased levels of glutamine/glutathione (Glu/GSH), unsaturated lipids (Lip_{unsat}), phosphocholine (PC), creatine (Cre) and UDP-sugars while lactate (Lac), phosphoethanolamine (PE) and choline (Cho) levels were decreased as compared to control cells. Metabolites for the discrimination of [**1**]-treated A2780 cells and HEK-293 cells from controls are indicated in the corresponding PLS-DA scores plots (Fig. 6C, D).

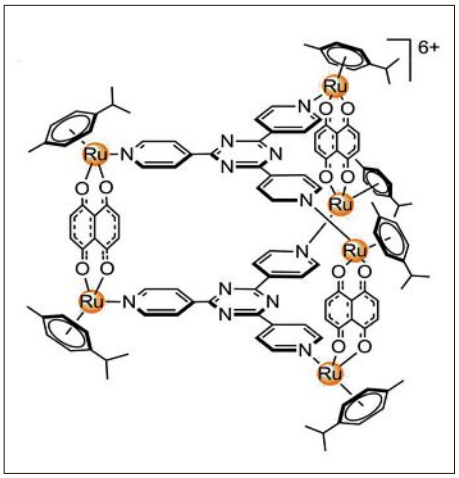

Fig. 5. Structure of the hexacationic ruthenium metallaprism $[(p\text{-cymene})_6Ru_6(tpt)_2(dhnq)_3]^{6+}$ ([**1**]). tpt: 2,4,6-tri(pyridin-4-yl)-1,3,5-triazine, dhnq: 5,8-dihydroxy-1,4-naphthoquinonato.[35]

Interestingly, cisplatin-sensitive and -resistant A2780 cells exhibited different metabolic responses to [**1**]. The strong overall decrease in lipids (all lipid resonances were affected) and simultaneous increase in choline-con-

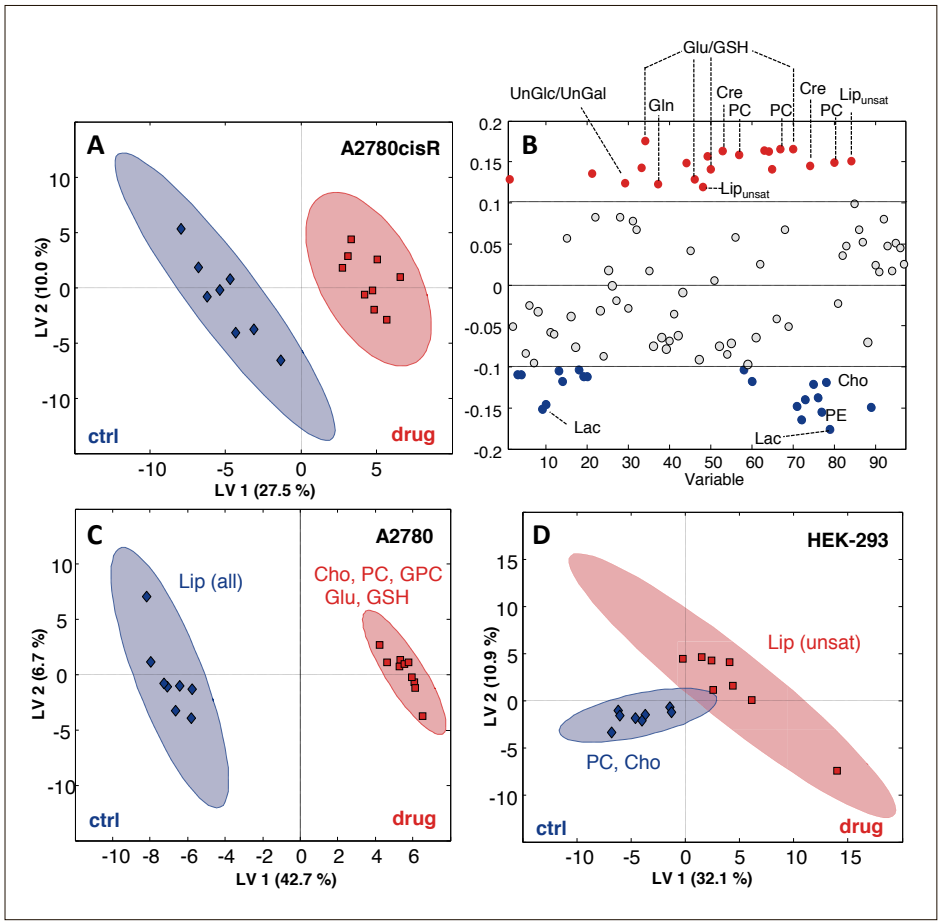

Fig. 6. PLS-DA scores plots for control cells (shown in blue) and cells treated with [**1**] (shown in red) for an incubation time of 24 h. A: A2780cisR cells, B: Loading plot for the first PLS-DA component LV 1 corresponding to the PLS-DA plot shown in A. Load values with high positive values are shown in red, and with high negative values are shown in blue. C: A2780 cells, D: HEK-293 cells. In C and D, metabolites with high load values are indicated in the plots. The 95% confidence ellipses are displayed for each group.

taining compounds in A2780 cells is an indicator of membrane breakdown, potentially associated with a necrotic cell death pathway.[43] On the contrary, the selective increase of unsaturated lipids as observed here for A2780cisR and HEK-293 cells, has been interpreted as indicator for the onset of an apoptotic cell death pathway.[26] The release of unsaturated fatty acids and phosphocholine from membrane phosphatidylcholines may be mediated by enhanced phospholipase activities[44] (Fig. 7). Upregulation of nucleotide sugars (see Figs. 3B and 7), which was even more pronounced after prolonged incubation with [**1**] in A2780cisR cells[35] indicated the involvement of glycosylation processes (Fig. 7). Interestingly, a similar response as observed for the ruthenium metallaprism in A2780cisR cells was found for cisplatin in non-resistant tumor cells, *i.e.* a simultaneous increase of unsaturated lipids and phosphate-sugar nucleotides.[28,45]

The ruthenium complex [**1**] was found to induce increased levels of glutamate (Glu)/glutathione (GSH) in all three cell lines at short and long incubation times. Glutathione, a tripeptide composed of the amino acids Cys, Glu, and Gly, plays key roles in protecting cells from oxidative damage and detoxification against xenobiotic compounds.[46] Resistance of cancer cells towards cisplatin has been related to the detoxification reaction with GSH due to an overexpression of the enzyme GSH-S-transferase (GST, Fig. 7).[47] The accumulation of GSH in the presence of [**1**] indicates that this resistance mechanism is not effective against the ruthenium complex. Further studies will be required to clarify if this is associated with an inhibition of GST or an increased supply of GSH by its stimulated biosynthesis.

Conclusion

HR-MAS NMR spectroscopy of biological semi-solid samples like cells and tissues is a powerful tool to study metabolic processes involving small metabolites in a most non-invasive way. It is particularly powerful when combined with multivariate statistical methods that simplify the quantitative analysis of complex metabolite spectra. Consequently, HR-MAS-based metabolomics has gained much interest in the study of cell responses towards drugs. Metabolite alterations may reflect stimulation either of biosynthetic or of catabolic pathways triggered by drug exposure. The changes provide indications for intracellular targets on the molecular basis and information on reactions involved in cell response. This knowledge may be useful for understanding cytotoxic mechanisms for a given compound as well as for tailoring more efficient drugs. Identification of specific biomarkers may act as indicators for early treatment response. The development of organometallic cytotoxic compounds has yielded numerous drug candidates with promising anticancer activity. However, for most of these metal-based compounds, the mechanisms of actions and their molecular targets are still unknown.[48] The application of HR-MAS-based metabolomics as a means to gain insights into living systems may prove useful to increase the knowledge in this field.

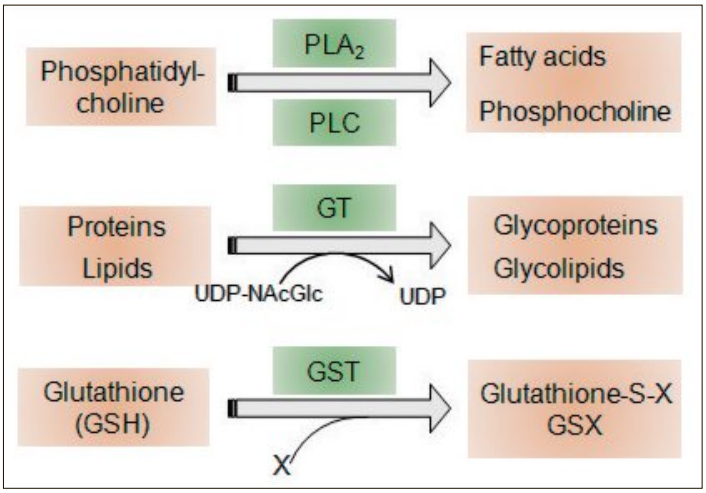

Fig. 7. Enzyme catalyzed intracellular reactions proposed to play a role in the cellular response towards treatment with [**1**]. PLA_2: Phospholipase A_2, PLC: Phospholipase C, GT: Glycosyl-Transferase, GST: GSH-S-Transferase, X: Xenobiotic compound.

Acknowledgements

Financial supports from the Department of Chemistry & Biochemistry at the University of Bern (JF) and from the Swiss National Science Foundation SNF grants # 206021-128736 (MV, PV), # 200021_149438 (MV, JF), and # 320030-138150 (PV) are gratefully acknowledged.

Received: February 5, 2017

[1] G. Jaouen, M. Salmain, 'Bioorganometallic Chemistry: Applications in Drug Discovery, Biocatalysis, and Imaging', Wiley-VCH Verlag GmbH & Co. KGaA: Weinheim, **2015**.
[2] G. Gasser, I. Ott, N. Metzler-Nolte, *J. Med. Chem.* **2011**, *54*, 3.
[3] C. G. Hartinger, N. Metzler-Nolte, P. J. Dyson, *Organometallics* **2012**, *31*, 5677.
[4] S. Medici, M. Peana, V. M. Nurchi, J. I. Lachowicz, G. Crisponi, M. A. Zoroddu, *Coord. Chem. Rev.* **2015**, *284*, 329.
[5] B. S. Murray, M. V. Babak, C. G. Hartinger, P. J. Dyson, *Coord. Chem. Rev*. **2016**, *306*, 86.
[6] S. J. Berners-Price, L. Ronconi, P. J. Sadler, *Progr. Nucl. Magn. Reson. Spectrosc.* **2006**, *49*, 65.
[7] K. J. Barnham, S. J. Berners-Price, Z. Guo, P. del Socorro Murdoch, P. J. Sadler, in 'Platinum and Other Metal Coordination Compounds in Cancer Chemotherapy 2', Eds. H. M. Pinedo, J. H. Schornagel, Springer US: Boston, MA, **1996**, pp 1-16.
[8] G. Lippens, M. Bourdonneau, C. Dhalluin, R. Warrass, T. Richert, C. Seetharaman, C. Boutillon, M. Piotto, *Curr. Org. Chem.* **1999**, *3*, 147.
[9] P. A. Keifer, *J. Org. Chem.* **1996**, *61*, 1558.
[10] J. Furrer, M. Piotto, M. Bourdonneau, D. Limal, G. Guichard, K. Elbayed, J. Raya, J. P. Briand, A. Bianco, *J. Am. Chem. Soc.* **2001**, *123*, 4130.
[11] A. Bianco, J. Furrer, D. Limal, G. Guichard, K. Elbayed, J. Raya, M. Piotto, J. P. Briand, *J. Comb. Chem.* **2000**, *2*, 681.
[12] K. Elbayed, M. Bourdonneau, J. Furrer, T. Richert, J. Raya, J. Hirschinger, M. Piotto, *J. Magn. Reson*. **1999**, *136*, 127.
[13] E. R. Andrew, A. Bradbury, R. G. Eades, *Nature* **1958**, *182*, 1659.
[14] W. P. Power, in 'Annual Reports on NMR Spectroscopy', Ed. G. A. Webb, Elsevier Academic Press Inc: San Diego, **2010**, Vol. 72, pp 111-156.
[15] C. Precht, G. Diserens, A. Oevermann, M. Vermathen, J. Lang, C. Boesch, P. Vermathen, *Biochim. Biophys. Acta, Mol. Cell Biol. Lipids* **2015**, *1851*, 1539.
[16] J. Martin-Sitjar, T. Delgado-Goni, M. E. Cabanas, J. Tzen, C. Arus, *Magn. Reson. Mater. Phys., Biol. Med.* **2012**, *25*, 487.
[17] J. C. Lindon, O. P. Beckonert, E. Holmes, J. K. Nicholson, *Progr. Nucl. Magn. Reson. Spectrosc.* **2009**, *55*, 79.
[18] O. Beckonert, M. Coen, H. C. Keun, Y. L. Wang, T. M. D. Ebbels, E. Holmes, J. C. Lindon, J. K. Nicholson, *Nat. Protoc.* **2010**, *5*, 1019.
[19] L. L. Cheng, 'Tissue and Cell Samples by HRMAS NMR. eMagRes', John Wiley & Sons, Ltd: **2007**.
[20] J. L. Griffin, J. P. Shockcor, *Nat. Rev. Cancer* **2004**, *4*, 551.
[21] J. K. Nicholson, J. C. Lindon, *Nature* **2008**, *455*, 1054.
[22] J. T. Bjerrum, 'Metabonomics, Methods and Protocols', Springer - Humana Press: **2015**, 1277.
[23] G. A. Nagana Gowda, D. Raftery, *Anal. Chem.* **2017**, *89*, 490.
[24] A. Zhang, H. Sun, H. Xu, S. Qiu, X. Wang, *OMICS* **2013**, *17*, 495.
[25] M. Bayet-Robert, D. Morvan, *PLoS ONE* **2013**, *8*, e57971.
[26] I. Lamego, I. F. Duarte, M. P. Marques, A. M. Gil, *J. Proteome Res.* **2014**, *13*, 6033.
[27] I. F. Duarte, I. Lamego, J. Marques, M. P. Marques, B. J. Blaise, A. M. Gil, *J. Proteome Res.* **2010**, *9*, 5877.
[28] X. Pan, M. Wilson, L. Mirbahai, C. McConville, T. N. Arvanitis, J. L. Griffin, R. A. Kauppinen, A. C. Peet, *J. Proteome Res.* **2011**, *10*, 3493.
[29] I. F. Duarte, A. F. Ladeirinha, I. Lamego, A. M. Gil, L. Carvalho, I. M. Carreira, J. B. Melo, *Mol. Pharmaceutics* **2013**, *10*, 4242.
[30] L. E. H. Paul, B. Therrien, J. Furrer, *J. Biol. Inorg. Chem.* **2012**, *17*, 1053.
[31] L. E. H. Paul, B. Therrien, J. Furrer, *Inorg. Chem*. **2012**, *51*, 1057.
[32] L. E. H. Paul, J. Furrer, B. Therrien, *J. Organomet. Chem.* **2013**, *734*, 45.
[33] L. E. H. Paul, B. Therrien, J. Furrer, *J. Biol. Inorg. Chem.* **2015**, *20*, 49.
[34] L. E. H. Paul, B. Therrien, J. Furrer, *Org. Biomol. Chem.* **2015**, *13*, 946.
[35] M. Vermathen, L. E. H. Paul, G. Diserens, P. Vermathen, J. Furrer, *Plos One* **2015**, *10*, e0128478.
[36] G. Diserens, D. Hertig, M. Vermathen, B. Legeza, C. E. Flück, J. M. Nuoffer, P. Vermathen, *Analyst* **2017**, *142*, 465.
[37] I. F. Duarte, J. Marques, A. F. Ladeirinha, C. Rocha, I. Lamego, R. Calheiros, T. M. Silva, M. P. M. Marques, J. B. Melo, I. M. Carreira, A. M. Gil, *Anal. Chem.* **2009**, *81*, 5023.
[38] D. S. Wishart, T. Jewison, A. C. Guo, M. Wilson, C. Knox, Y. Liu, Y. Djoumbou, R. Mandal, F. Aziat, E. Dong, S. Bouatra, I. Sinelnikov, D. Arndt, J. Xia, P. Liu, F. Yallou, T. Bjorndahl, R. Perez-Pineiro, R. Eisner, F. Allen, V. Neveu, R. Greiner, A. Scalbert, *Nucleic Acids Res*. **2012**, *41*, D801.
[39] S. D. Wishart, R. Mandal, A. Stanislaus, M. Ramirez-Gaona, *Metabolites* **2016**, *6*, 1.
[40] G. Diserens, M. Vermathen, I. Gjuroski, S. Eggimann, C. Precht, C. Boesch, P. Vermathen, *Anal. Bioanal. Chem.* **2016**, *408*, 5651.
[41] M. Bayet-Robert, D. Loiseau, P. Rio, A. Demidem, C. Barthomeuf, G. Stepien, D. Morvan, *Magn. Reson. Med.* **2010**, *63*, 1172.
[42] A. H. Zhang, H. Sun, S. Qiu, X. J. Wang, *Magn. Reson. Chem.* **2013**, *51*, 549.
[43] J. M. Hakumäki, R. A. Kauppinen, *Trends Biochem. Sci.* **2000**, *25*, 357.
[44] J. M. Hakumäki, H. Poptani, A. M. Sandmair, S. Yla-Herttuala, R. A. Kauppinen, *Nat. Med.* **1999**, *5*, 1323.
[45] X. Pan, M. Wilson, C. McConville, T. N. Arvanitis, J. L. Griffin, R. A. Kauppinen, A. C. Peet, *Metabolomics* **2013**, *9*, 722.
[46] H. J. Forman, H. Zhang, A. Rinna, *Mol. Aspects Med.* **2009**, *30*, 1.
[47] D. J. Stewart, *Crit. Rev. Oncol./Hematol.* **2007**, *63*, 12.
[48] S. Spreckelmeyer, C. Orvig, A. Casini, *Molecules* **2014**, *19*, 15584.